Journal of Alloys and Compounds 488 (2009) 306–309

Contents lists available at ScienceDirect

Journal of Alloys and Compounds

journal homepage: www.elsevier.com/locate/jallcom

Electrical investigation of the compound: $LiFe_{2/5}Ni_{3/10}Co_{3/10}VO_4$

Moti Ram*

Department of Physics and Meteorology, Indian Institute of Technology, Kharagpur, West Bengal 721302, India

ARTICLE INFO

Article history:
Received 11 June 2009
Received in revised form 17 August 2009
Accepted 18 August 2009
Available online 31 August 2009

Keywords:
Ceramics
Chemical synthesis
Complex electrical impedance
Electrical conductivity

ABSTRACT

The $LiFe_{2/5}Ni_{3/10}Co_{3/10}VO_4$ ceramics has been produced by solution-based chemical route. Orthorhombic unit cell structure of the compound is selected by X-ray diffraction study. Complex impedance spectroscopy (CIS) technique has been used to study the electrical properties. Complex impedance analysis shows: (i) grain interior, grain boundary and electrode–material interface contributions to electrical response and (ii) the presence of temperature dependent electrical relaxation phenomena in the material. Temperature dependence of dc and ac conductivity indicates that electrical conduction in the material is a thermally activated process. Frequency dependence of σ_{ac} at different temperatures obeys Jonscher's universal power law governed by the relation: $\sigma_{ac} = \sigma_{dc} + A\omega^n$.

1. Introduction

In recent years, spinel structure materials have been investigated extensively due to their useful physical and chemical properties and applications in preparing magnetic cores, information storage systems, magnetic fluids, microwave absorbers and medical diagnostics, etc. [1–3]. Different types of spinels can be formed on the basis of oxidation state of the cations, namely: (4, 2) type such as $TiMg_2O_4$ (2, 3) type such as $MgAl_2O_4$ (1, 3, 4) type such as $LiAlTiO_4$ (1, 6) type such as Na_2WO_4 (1, 2, 5) type such as $LiNiVO_4$, and (1, 3) type such as $Li_{0.5}Al_{2.5}O_4$. The distribution of cations in tetrahedral and octahedral sites leads to two extreme situations. One of them is normal spinel in which the divalent cations are situated in the tetrahedral sites (e.g. $MgAl_2O_4$) and the other one is inverse spinel in which the divalent cations occupy half of the octahedral sites and the tetrahedral sites are occupied by the trivalent cations (e.g. $MgFe_2O_4$) [4,5]. This distribution of cations can be modified by means of adequate changes in chemical composition which shows the changes in physical and chemical properties of the resulting materials [6]. The mechanism of electrical properties in spinels depends on the arrangement of ions in different sites. Electrical properties of spinel compounds such as $LiFe_{1/2}Co_{1/2}VO_4$, Li_xMVO_4 (M = Ni, Co; $x = 0.8, 1.0, 1.2$), $LiFeTiO_4$, etc. are studied by different researchers [7–10]. This has motivated me for the formation of a spinel compound ($LiFe_{2/5}Ni_{3/10}Co_{3/10}VO_4$) and to study its electrical properties. The $LiFe_{2/5}Ni_{3/10}Co_{3/10}VO_4$ compound is mechanically strong and environment friendly. Complex impedance spectroscopy (CIS) is a nondestructive method to study the electrical properties of such materials [11]. It correlates the microstructural and electrical properties of polycrystalline oxide materials. According to this method, when an ac input signal is applied across sample, the output response appears as semicircles in the complex plane plots that represents electrical phenomena due to the bulk material, grain boundary effect and interfacial polarization [11,12]. In the present paper, structural, microstructural and electrical properties of $LiFe_{2/5}Ni_{3/10}Co_{3/10}VO_4$ compound are discussed. Electrical properties are studied by ac technique of CIS. Crystal structure is examined by X-ray diffraction method.

2. Experimental details

Solution-based chemical method was used to prepare $LiFe_{2/5}Ni_{3/10}Co_{3/10}VO_4$ fine powder. The stoichiometric amount of highly pure $LiNO_3$, $Ni(NO_3)_2{\cdot}6H_2O$, $Co(NO_3)_2{\cdot}6H_2O$, $FeCO_3$ and NH_4VO_3 was dissolved in distilled water and mixed together. $FeCO_3$ was dissolved in warm distilled water in the presence of oxalic acid. After sometime triethanolamine (TEA) was added maintaining a ratio of 3:1 with metal ions. HNO_3 and oxalic acid were added to dissolve the precipitation and then the clear solution was evaporated at ~200 °C temperature with continuous stirring. A fluffy, mesoporous and carbon-rich precursor mass was formed by complete evaporation of the solution. After grinding, the voluminous, fluffy and black carbonaceous mass was calcined at 550 °C for 3 h to produce the desired phase. That is confirmed by X-ray diffraction analysis using a diffractometer (PANalytical PW 3040/60 X'Pert PRO) in the angle range ($20° \le 2\theta \le 80°$) on being irradiated by CuKα (1.5419 Å). The calcined powder was cold pressed into circular disc shaped pellet of diameter (12–13 mm) of various thicknesses with polyvinyl alcohol as the binder using hydraulic press at a load of ~3–4 tonnes. These pellets were then sintered at 575 °C for 2 h followed by slow cooling process. The surface morphology of the gold-sputtered pellet was recorded with different magnifications at room temperature using a ZEISS (Model: SUPRA™ 40) field emission scanning electron microscope. Subsequently, the pellets were polished by fine emery paper to make their faces smooth and parallel. The pellets were finally coated with conductive silver paint and dried at 150 °C for 3 h before carrying out electrical measurements. Electrical measurements were made by applying a voltage of ~0.701 V using a computer-

* Tel.: +91 3222281902.
E-mail address: motiram05@yahoo.co.in.

0925-8388/$ – see front matter © 2009 Elsevier B.V. All rights reserved.
doi:10.1016/j.jallcom.2009.08.111

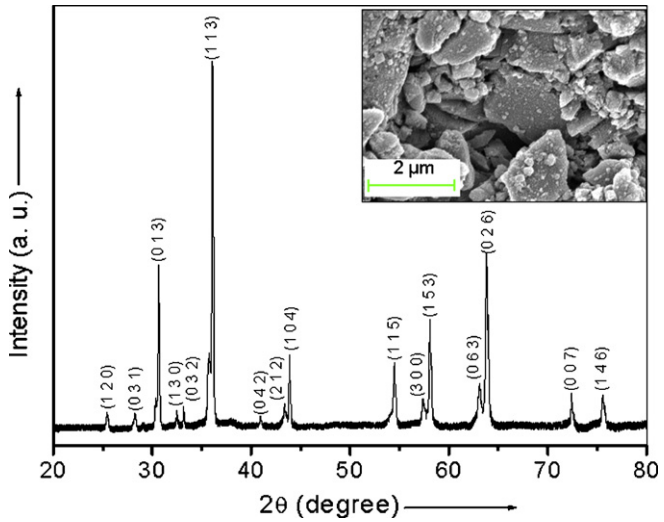

Fig. 1. X-ray diffraction pattern and field emission scanning electron micrograph (inset) of $LiFe_{2/5}Ni_{3/10}Co_{3/10}VO_4$ at room temperature.

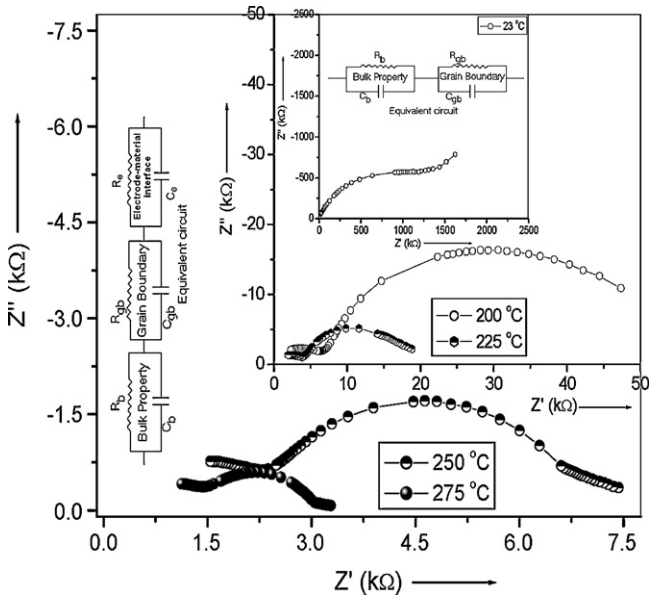

Fig. 2. Nyquist plots at different temperatures with electrical equivalent circuit (inset).

controlled frequency response analyzer (HIOKI LCR Hi TESTER, Model: 3532-50) with varying temperature over the range of frequencies (10^2–10^6 Hz).

3. Results and discussion

3.1. Structure/microstructure

Fig. 1 displays X-ray diffraction (XRD) pattern of $LiFe_{2/5}Ni_{3/10}Co_{3/10}VO_4$ at room temperature. The XRD data are analyzed using standard computer software (POWD MULT) [13] and they confirm an orthorhombic unit cell structure of the compound with lattice parameters of $a = 4.8180$ Å, $b = 10.0883$ Å and $c = 9.1356$ Å. The lattice parameters are refined by a least squares refinement method.

The microstructure of the sintered pellet of the material is examined by the field emission scanning electron microscopy (FE-SEM). Fig. 1 (inset) shows a field emission scanning electron micrograph

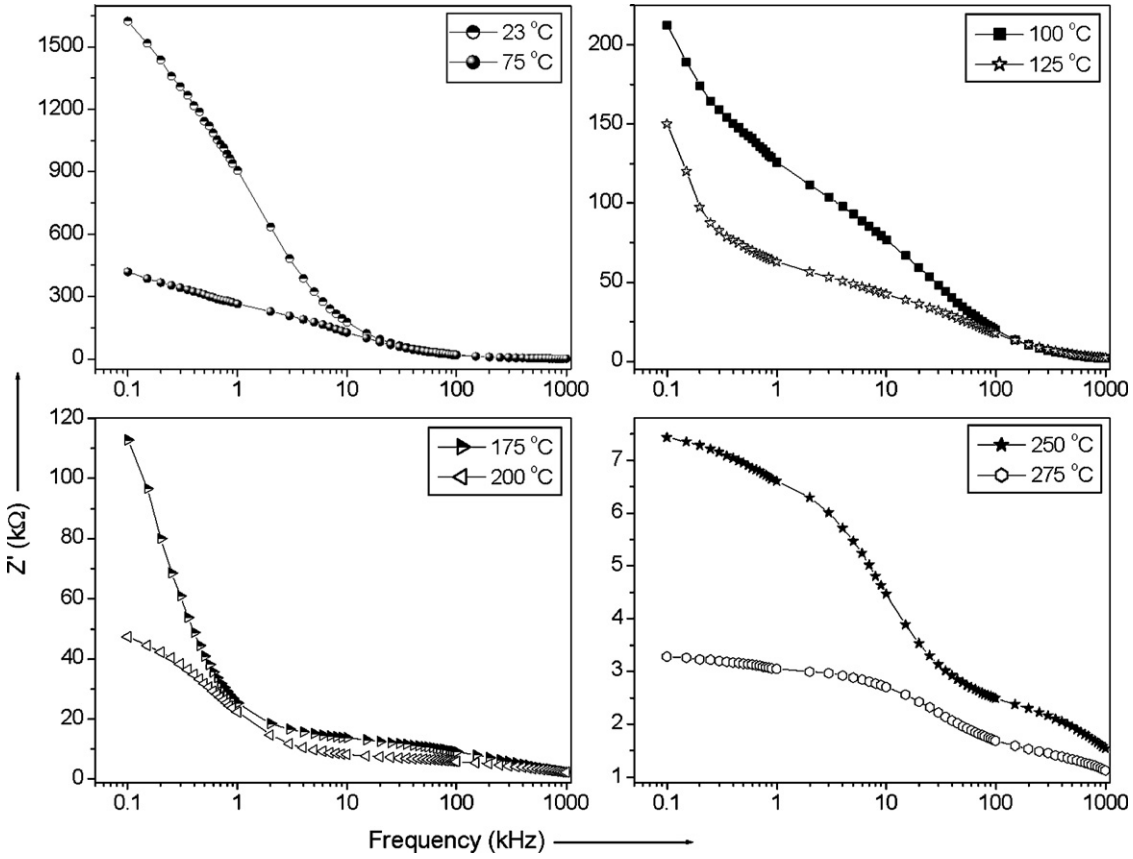

Fig. 3. Frequency dependence of Z' at different temperatures.

at room temperature of the material's sintered pellet, it clearly indicates a polycrystalline texture of the material. Micrograph also reveals that grains of unequal sizes (~0.1–2 μm) are homogeneously distributed on the surface of the sample. The grain size (~0.1–2 μm) of $LiFe_{2/5}Ni_{3/10}Co_{3/10}VO_4$ prepared by solution-based chemical method is smaller than that of the grain size (1–3 μm) of $LiFe_{1/2}Co_{1/2}VO_4$ that is prepared by conventional solid state route [7].

3.2. Complex electrical impedance

Complex impedance plots of $LiFe_{2/5}Ni_{3/10}Co_{3/10}VO_4$ at different temperatures are given in Fig. 2. It shows semicircles at studied temperatures. These semicircles are not perfect semicircles but skewed (inclined) with their centers depressed below the real (Z') axis by an angle $(n-1)\pi/2$, where n lies between 0 and 1 [14]. It indicates the presence of non-Debye type relaxation phenomena in the material that conforms to a distribution of relaxation time. The diameter of the semicircle decreases as temperature increases and indicates reduce in resistive behavior of the material. The presence of double semicircular arcs up to 225 °C indicates that electrical processes in the material are taking place due to bulk property and grain boundary effects and modeled by two parallel RC elements in series. The presence of third semicircular arc in the pattern at $T \geq 250$ °C is due to the polarization effects (polarization at the electrode–material interface) and modeled by three parallel RC elements in series [11].

Frequency dependence of Z' at different temperatures is shown in Fig. 3. The value of Z' decreases with rise in both frequency and temperature, which indicates an increase in ac conductivity with increasing temperature and frequency [15]. Frequency dependence of Z'' at different temperatures is shown in Fig. 4. The pattern shows dispersion at low frequencies. The Z'' maxima are observed in the pattern that appears to shift towards the high frequency side with rise in temperature indicating temperature dependence of the relaxation time. Further, the occurrence of maxima (peak) at different frequencies indicates multiple relaxations [12]. A merge of these curves at the higher frequencies indicates the depletion of release of space charges at those frequencies. The relaxation time (τ) is evaluated using the equation: $\tau = 1/2\pi f_{max}$, where f_{max} is the peak frequency (or relaxation frequency) corresponding to Z'' maxima (peak). The log (τ) versus $10^3\,T^{-1}$ plot is represented in Fig. 5. It follows the Arrhenius relation [$\tau = \tau_0 \exp(-E_a/kT)$], where τ_0 = pre-exponential factor, E_a = activation energy, k = Boltzmann constant and T is absolute temperature [16]. The activation energy

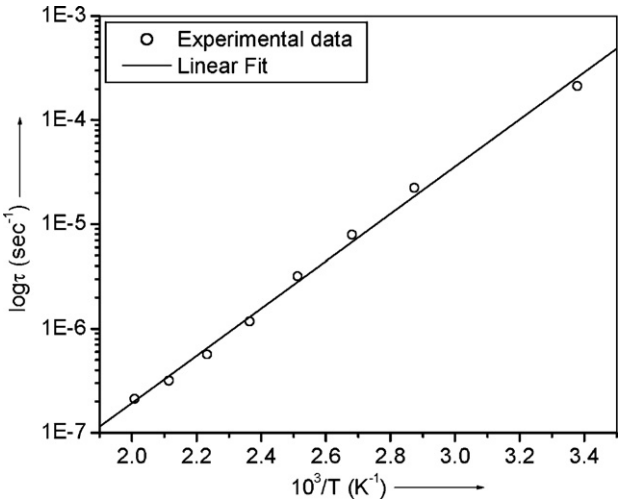

Fig. 5. Variation of relaxation time (τ) as a function of temperature.

(E_a) is calculated from the slope of this plot as ~(0.450 ± 0.012) eV (23–225 °C).

3.3. Electrical conductivity

The variation of dc conductivity (σ_{dc}) as a function of temperature is given in Fig. 6. Here σ_{dc} increases as temperature rises and follows straight line (Arrhenius) nature. This behavior can be explained by using the relation: $\sigma = \sigma_o \exp[-E_a/kT]$, where σ_0 = pre-exponential factor corresponding to $1/T = 0$, E_a = activation energy for charge transfer and k = Boltzmann constant [16]. These features suggest that the electrical conduction in the material is a thermally activated process. The activation energy (E_a) estimated from this plot is ~(0.426 ± 0.007) eV (50–300 °C). It is in good agreement with E_a as estimated from Fig. 5. Furthermore, E_a of $LiFe_{2/5}Ni_{3/10}Co_{3/10}VO_4$ is greater than that of E_a (~0.38 eV) of $LiFe_{1/2}Co_{1/2}VO_4$ [7,8]. This indicates a difference in the energy barrier for the charge carriers to overcome it [17].

Frequency dependence of ac conductivity (σ_{ac}) at different temperatures is displayed in Fig. 7(a). The plots indicate a frequency-independent plateau at low frequencies which is corresponding to dc conductivity. It is extending towards high frequency side with rise in temperature. The change in slope is observed in the plots. The frequency at which change in slope (i.e. disper-

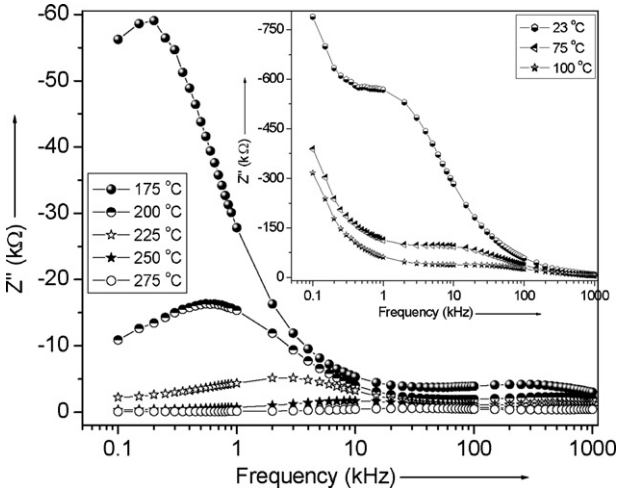

Fig. 4. Frequency dependence of Z'' at different temperatures.

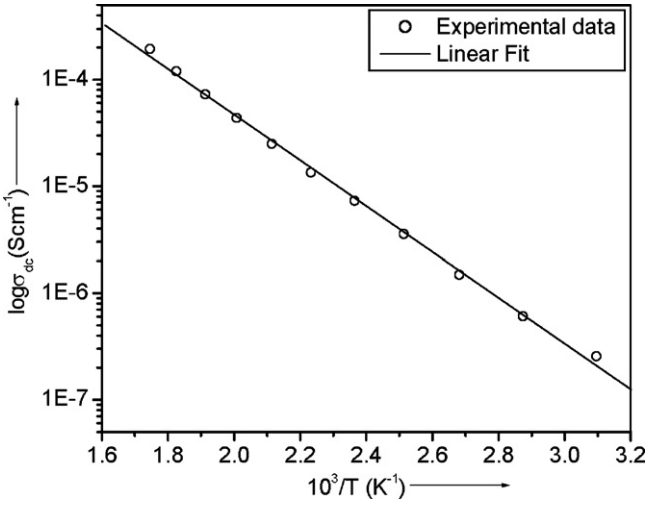

Fig. 6. Variation of σ_{dc} as a function of temperature.

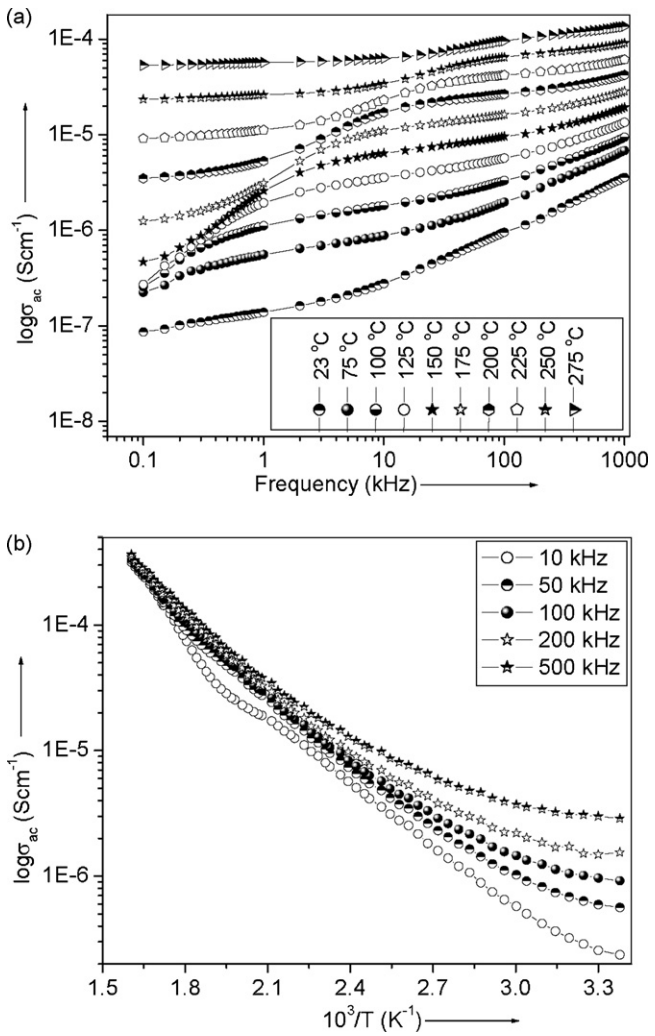

Fig. 7. Frequency dependence of σ_{ac} at different temperatures (Fig. a), and temperature dependence of σ_{ac} at different frequencies (Fig. b).

sion) takes place is known as hopping frequency and it corresponds to polaron hopping of charged species. This hopping frequency is shifting towards higher frequencies with rise in temperature. These features suggest hopping type mechanism for electrical conduction in the material that is governed by the Jonscher's power equation: $\sigma_{ac} = \sigma_{dc} + A(\omega)^n$ [18], where n is the frequency exponent in the range of $0 \leq n \leq 1$ and A is a constant that depends upon temperature. Also, σ_{ac} increases with rise in temperature which signifies that the electrical conduction in the material is a thermally activated process.

Fig. 7(b) presents the temperature dependence of σ_{ac} at different frequencies. The σ_{ac} increases with rise in temperature that indicates electrical conduction in the material as thermally activated process. It obeys an empirical relation: $\sigma_{ac} = \sigma_o \exp[-E_a/kT]$, where σ_o = pre-exponential factor, E_a = activation energy and k = Boltzmann constant [18]. Conduction may be due to electrons in low temperature region and oxygen vacancies at higher temperatures [18]. Further, the merger of all curves at high temperatures is due the intrinsic conductivity of the materials in this temperature range [19].

4. Conclusions

Solution-based chemical method has been used to produce $LiFe_{2/5}Ni_{3/10}Co_{3/10}VO_4$ ceramics whose XRD study shows an orthorhombic unit cell structure with lattice parameters of $a = 4.8180$ Å, $b = 10.0883$ Å and $c = 9.1356$ Å. FE-SEM image indicates grains of unequal sizes (~0.1–2 μm) are distributed homogeneously throughout the sample. Grain interior, grain boundary and electrode–material interface contributions to electrical response is identified by complex impedance plots. A detailed electrical conductivity study indicates that electrical conduction in the material is a thermally activated process.

Acknowledgements

The author is grateful to the Ferroelectrics Laboratory of the Department of Physics & Meteorology, Nanomaterials Laboratory of the Department of Chemistry and Central Research Facility, Indian Institute of Technology, Kharagpur-721302 (W.B.), India for providing facilities to conduct experiments.

References

[1] A. Bayka, N. Kasapoglu, Y. Koseoglu, A.C. Basaran, H. Kavas, M.S. Toprak, Cent. Eur. J. Chem. 6 (2008) 125.
[2] G. Lorenzi, G. Baldi, D.F. Benedetto, V. Faso, P. Lattanzi, M. Romanelli, J. Eur. Ceram. Soc. 26 (2006) 317.
[3] A.L. Fernandez, L. Pablo, Pigment Resin Technol. 31 (2002) 350.
[4] N.M. Deraz, M.M. Hessien, J. Alloys Compd. 475 (2009) 832.
[5] K.E. Sickafus, J.M. Wills, N.W. Grimes, J. Am. Ceram. Soc. 82 (1999) 3279.
[6] V.V. Boldyrev, Reactivity of Solids: Past, Present and Future, Blackwell, Oxford, 1996.
[7] M. Ram, R.N.P. Choudhary, A.K. Thakur, Mater. Lett. 60 (2006) 2824.
[8] M. Ram, S. Chakrabarti, J. Alloys Compd. 462 (2008) 214.
[9] S. Selvasekarapandian, M.S. Bhuvaneswari, S. Fujihara, S. Koji, Acta Mater. 54 (2006) 1767.
[10] M.A. Arillo, M.L. Lopez, E. Perez-Cappe, C. Pico, M.L. Veiga, Solid State Ionics 107 (1998) 307.
[11] J.R. Macdonald, Impedance Spectroscopy: Emphasizing Solid State Material and Systems, Wiley, New York, 1987.
[12] S. Sen, R.N.P. Choudhary, A. Tarafdar, P. Pramanik, J. Appl. Phys. 99 (2006) 1241141.
[13] E. Wu, POWD MULT: An Interactive Powder Diffraction Data Interpretation and Indexing Program, Version 2.1, School of Physical Sciences, Flinder University of South Australia, Bardford Park, SA, Australia, 1989.
[14] A.R. James, S. Balaji, S.B. Krupanidhi, Mater. Sci. Eng. B 64 (1999) 149.
[15] A.M.M. Farea, S. Kumar, K.M. Batoo, A. Yousef, C.G. Lee, Alimuddin, J. Alloys Compd. 464 (2008) 361.
[16] A. Hassib, A. Razik, Solid State Commun. 147 (2008) 345.
[17] C.H. Song, H.W. Park, H.W. Choi, M. Kim, Y.S. Yang, J. Korean Phys. Soc. 49 (2006) S465.
[18] S. Kumar, K.B.R. Varma, Solid State Commun. 146 (2008) 137.
[19] K.S. Rao, D.M. Prasad, P.M. Krishna, B. Tilak, K.C. Varadarajulu, Mater. Sci. Eng. B 133 (2006) 141.